PREPRINTS #62

OF THE

STEWARD OBSERVATORY

THE UNIVERSITY OF ARIZONA
TUCSON, ARIZONA 85721, U.S.A.

DIFFRACTION EFFECTS IN PULSATING RADIO SOURCES

F.A. Hopf
Optical Sciences Center, University of Arizona

and

W.J. Cocke and N.D. Lubart
Steward Observatory, University of Arizona

DIFFRACTION EFFECTS IN PULSATING RADIO SOURCES

F. A. Hopf*

Optical Sciences Center, University of Arizona

and

W. J. Cocke and N. D. Lubart+

Steward Observatory, University of Arizona

ABSTRACT

A pulsar radio emission model is developed to explore the effects of diffraction on pulsar beaming. At very low frequencies ($\nu < 10$ MHz), we predict an increase of pulse width and the discovery of new pulsars. The pulse width increase would be very difficult to untangle from interstellar scintillation effects. Observation of these diffraction effects would place restrictions on the size and radius of curvature of the emission regions.

---

*Supported by Kirtland Air Force Base (AFWL).

+Present address: IBM Corporation, Essex Junction, Vermont.

I. INTRODUCTION

It is now a nearly universal presumption among astronomers that the pulsar phenomenon is due to neutron stars that are emitting directional radiation and are simultaneously rotating. We observe, then, periodic bursts of electromagnetic radiation in the same way that we see periodic flashes of light from a lighthouse. This kind of beaming must exhibit an edge effect from diffraction that is an exact counterpart to the resolution capability of a telescope; namely, that just as the aperture size of a telescope limits its resolution, the size of the emitting region of a pulsar limits the collimation of the beamed radio emission. This is not an _a priori_ statement about pulsar structure, but rather a basic property of electromagnetic waves.

Thus the observation of beamed radiation carries with it certain necessary consequences, and it is the purpose of this note to explore the possible observational significance of these consequences. For simplicity we limit ourselves to a model of the emitting region of the pulsar such that there is a surface of fixed radius d and radius of curvature R, with which the wavefronts are conformal. As we shall see, this model is consistent with presently observed properties of pulsar radiation and leads to interesting and possibly observable effects at very low frequencies ($\nu < 10$ MHz). The observation of these diffraction effects would lead directly to a determination of d and R. In addition, we conclude that there are many pulsars which remain to be discovered at low frequencies.

II. THE GAUSSIAN MODEL

The phenomenon of diffraction is a consequence of Maxwell's equations and represents a transformation of the wave from one location in space to another. This is in general a complicated affair, but for our model the appropriate approximation is that of a Gaussian beam, which can be obtained by transforming the monochromatic spherical wave solution e^{ikr}/r by the substitution $x \to x$, $y \to y$, $z \to z - iz_o$, where z_o is a length parameter such that the beam radius is

$$w(z) = w_o(1+z^2/z_o^2)^{1/2} \quad (1),$$

with $z_o = \pi w_o^2/\lambda$, λ being the wavelength of the radiation (Gordon 1968). The beam propagates in the z-direction.

The Gaussian approximation consists in assuming $\rho^2 \equiv x^2+y^2 << z^2+z_o^2$, so that the angular diameter of the beam is small, as is certainly the case for pulsar radiation. In this case the amplitude of the wave is approximately

$$|\underset{\sim}{E}| \simeq \frac{V_o}{w(z)} \exp[-\rho^2/w(z)^2] \quad (2),$$

and the radius of the curvature of the wave fronts is

$$R(z) \simeq z^{-1}(z^2+z_o^2) \quad (3).$$

These equations describe the monochromatic radio beam propagating in the z-direction. It is shown schematically in Figure 1, in which the wave fronts and beam radius w(z) are delineated. Note that at the minimum radius ($w = w_o$), the wave surface is flat. The asymptotic angular spread θ_D of the beam is called the diffraction angle and is defined by the relation

$$\tan \theta_D \equiv \lim_{z\to\infty} \frac{w(z)}{z} = \frac{w_o}{z_o} = \frac{\lambda}{\pi w_o} \quad (4).$$

Note that if an object is emitting from a plane surface, then the knowledge of θ_D and λ is enough to predict the radius (w_o) of the emitting region. This inference is more complicated if one supposes that the radiation is emitted from one of the surfaces of finite radius of curvature, since the behavior of the radiation depends on the assumed radius of curvature. For our pulsar model, we assume that the polychromatic emission is characterized by a radius d and radius of curvature R which do not depend on λ, and that the wavefronts are all conformal with this curved emission surface.

We may then let $z = 0$ represent the center of curvature of the emission region and $z = z_c$ be the z-coordinate of the beam waist; i.e., the virtual location of the minimum diameter of the beam. This is shown in Figure 2, where we include the hyperbolae that define the beam diameters. Equations (1) and (3) then imply $d = w_o[1+(R-z_c)^2/z_o^2]^{1/2}$ and $R = (R-z_c)^{-1}[(R-z_c)^2+z_o^2]$, where z_c and w_o depend on λ. These two relations may be used to find the polychromatic beaming angle

$$\tan\theta_{D\lambda} = \frac{\lambda}{\pi d}\left(1+\frac{d^4\pi^2}{R^2\lambda^2}\right)^{1/2} \simeq \theta_{D\lambda} \qquad (5).$$

In the short wavelength limit we have $\theta_{D0} \simeq d/R \equiv \theta_N$, which we call the natural or geometric beaming angle of the pulsar. For λ very large, on the other hand, we obtain $\theta_{D\infty} \simeq \lambda/\pi d \equiv \theta_\infty$.

Thus at short wavelengths the model radiates in the fixed geometric beam, and at large wavelengths the radius of curvature of the emitting surface is not important.

For arbitrary wavelengths we may obviously write eqn. (5) as

$$\theta_{D\lambda} \simeq (\theta_\infty^2+\theta_N^2)^{1/2} \qquad (6).$$

III. PULSAR SPECTRA AND PULSE WIDTHS

We now compute a pulsar spectral intensity correction factor g_ν and a pulse width ΔP using the theory developed in the preceeding section. We assume that the beam diameter is small compared to the angular distance ϕ_o from the center of the beam to the pulsar rotation axis. The line-of-sight to the observer then scans across the beam at an angular distance θ_o from the beam center. If the angular rotational velocity of the pulsar is Ω rad sec^{-1}, the apparent linear beam velocity at distance z is $v \simeq z\Omega\sin\phi_o$, so that $x = vt = z\Omega t\sin\phi_o$ (see Figure 3).

Then from eqn. (2) the observed spectral radiation intensity as a function of time may be written, with $y/z \simeq \theta_o$, and $z \gg z_o$,

$$F_\nu(t) \propto |\underset{\sim}{E}|^2 \simeq f_\nu z^{-2}\theta_{D\lambda}{}^{-2}\exp[-2(\theta_o{}^2+\Omega^2 t^2\sin^2\phi_o)/\theta_{D\lambda}{}^2] \qquad (7),$$

where f_ν is an intrinsic spectral intensity.

It follows that the pulse width ΔP is $\theta_{D\lambda}/\Omega\sin\phi_o$, or

$$\Delta P/P = (\theta_N{}^2+\theta_\infty{}^2)^{1/2}/(2\pi\sin\phi_o) \qquad (8).$$

For small λ, $\Delta P/P \simeq d/(2\pi R\sin\phi_o)$, and for large λ, $\Delta P/P \simeq \lambda/(2\pi^2 d\sin\phi_o)$. Note that there is a characteristic wavelength $\lambda_c \equiv \pi d^2/R$ where $\Delta P(\lambda)$ begins to turn upward as a function λ.

We may also integrate eqn. (7) with respect to time to obtain a total pulse intensity

$$F_\nu{}^o \simeq \int_{-\infty}^{+\infty} F_\nu(t)\,dt = \frac{f_\nu\exp(-2\theta_o{}^2/\theta_{D\lambda}{}^2)}{z^2\theta_{D\lambda}\Omega\sin\phi_o} = \frac{f_\nu g_\nu}{\theta_N z^2\Omega\sin\phi_o},$$

defining $g_\nu \equiv \exp(-2\theta_o{}^2/\theta_{D\lambda}{}^2)\theta_N/\theta_{D\lambda}$. In Figure 4 we plot log g_ν as a function of log (ν/ν_c), where $\nu_c \equiv c/\lambda_c = cR/(\pi d^2)$ is the characteristic frequency. We plot three cases, for θ_o equal to $1/2\theta_N$, θ_N and $2\theta_N$. Note the sharp high-frequency cutoff for $\theta_o > \theta_N$. There is also a first-power drop-off at low frequencies.

In summary, then, the observational consequences of diffraction are, first, a broadening of the pulse, and, second, a modification of the intrinsic spectrum as shown in Fig. 4. In the next section we show the implications that would follow from a detection of these effects, and we also discuss the difficulties associated with observations at such low frequencies.

IV. APPLICATION AND DISCUSSION

Observations show that many pulsars exhibit very little change in pulse width as a function of frequency. For example, one may refer to measurements by Lyne, Smith, and Graham (1971) at 151, 240, 408, and 610 MHz, and by Manchester (1971) at 410 and 1665 MHz, where one sees many pulse widths that are constant within the accuracy of the observations. There are many pulsars whose pulse widths even appear to decrease slightly at longer wavelengths (Manchester 1971, Tables 1 and 2), but the reality of this trend is not certain.

This rough constancy of $\Delta P/P$ with wavelength is consistent with our Gaussian beam model if we suppose that $\lambda_{obs} < \lambda_c$, and is strong evidence in favor of its being a good representation of the real case. Then generally we are inside the geometric cone, where $\Delta P/P \simeq d/(2\pi R\sin\phi_o)$. Typically, $\Delta P/P \simeq 2 \times 10^{-2}$ so that $d/R \simeq 0.1 \sin\phi_o \simeq 7 \times 10^{-2}$.

Now, for any emission region associated with a neutron star or its magnetosphere, we should have $R \gtrsim 10^6$ cm, and therefore $d \gtrsim 7 \times 10^4$ cm. This implies $\lambda_c \gtrsim 1.5 \times 10^4$ cm, or $\nu_c = c/\lambda_c \lesssim 2$ MHz.

Measurements from outside the earth's ionosphere could be made in this frequency region, and for some pulsars the characteristic dependence of ΔP on λ given by eqn. (8) might be observed. Let us suppose that we characterize an observed $\Delta P(\lambda)$ diffraction curve by three observational parameters, $O_1 \equiv \Delta P(0)/P = d/(2\pi R\sin\phi_o)$, $O_2 \equiv \lambda_c \equiv \pi d^2/R$, and $O_3 \equiv \lim_{\lambda\to\infty} \frac{\Delta P(\lambda)}{P\lambda} = (2\pi^2 d\sin\phi_o)^{-1}$. Then one can easily show that O_1, O_2, and O_3 are not independent, but must satisfy the relation $O_1 = O_2 O_3$. This would serve as a check on the theory if an asymptotically linear increase of ΔP with λ were observed.

The three unknowns of interest are ϕ_o, d, and R. For rough estimation from observation we set $\sin\phi_o \simeq 1$, whereupon d and R may be found as $d \simeq O_2/(2\pi^2 O_1)$ and $R \simeq O_2/(4\pi^3 O_1{}^2)$. Thus if there were no complicating effects one could determine observationally both the diameter and radius of curvature of the emitting region.

We must caution, however, that at these very low frequencies interstellar scintillation would almost completely mask these pulse broadening effects in the majority of pulsars, since one expects a very strong dependence of ΔP on λ from scintillation (Salpeter 1969). For example, Sutton (1971) has noted that $\Delta P(\lambda) \propto \lambda^4$ for some pulsars. However, it might be possible to subtract out the scintillation effects in some cases, since scintillation broadening affects primarily the trailing edges of the pulses.

Komesaroff, Hamilton, and Ables (1972) have measured the characteristics of the pulsar PSR 0833-45 and find that its scintillation properties may be caused by scattering in a localized region of dimensions much smaller than the total distance to the pulsar. This region is presumably the Gum Nebula. This suggests that there may be some pulsars for which such broadening is, relatively speaking, very small and for which diffraction effects at low frequencies may be observable, although perhaps only as small corrections to scintillation broadening.

Of great interest is the plot of the spectral intensity correction factor g_ν, depicted in Figure 4, where we note that for $\theta_o > \theta_N$ there is a very strong "high-frequency" cutoff. This implies that there may be some pulsars which are unobservable for $\nu > \nu_c$ and which may yet be discovered at these low frequencies.

The discovery of such diffraction effects in the frequency regime around 1 MHz would be of great interest, since it would imply $R \simeq 10^6$cm, indicating that the emission region is near the neutron star surface. However, if the emission takes place near the velocity-of-light cylinder, then probably $10^8 \lesssim R \lesssim 10^{10}$, with $\nu_c \lesssim 20$ kHz, which would be completely unmanageable observationally.

REFERENCES

Gordon, J. P. 1968, in Laser Technology and Applications (New York: McGraw-Hill), p. 38.

Komesaroff, M. M., Hamilton, P. A., and Ables, J. G. 1972, Aust. J. Phys., 25, 759.

Lyne, A. G., Smith, F. G., and Graham, D. A. 1971, M.N.R.A.S., 153, 337.

Manchester, R. N. 1971, Ap. J. Suppl., 23, 283.

Salpeter, E. E. 1969, Nature, 221, 31.

Sutton, J. M. 1971, M.N.R.A.S., 155, 51.

FIGURE CAPTIONS

Fig. 1 - The half-width surface (a hyperboloid of one sheet) and wave fronts of the monochromatic Gaussian beam. w_o is the beam-waist radius and θ_D is the diffraction angle.

Fig. 2 - The polychromatic Gaussian model. All wave fronts are conformal with the fixed spherical cap of radius of curvature R and radius d. $\theta_{D\lambda}$ is the polychromatic diffraction angle, and θ_N is its short wavelength limit.

Fig. 3 - Definition of the angles ϕ_o, the angle between the beam direction and the rotation axis, and θ_o, the minimum angle between the beam direction and the direction to the observer.

Fig. 4 - The spectral energy correction factor g_ν as a function of θ_o and frequency ν in units of the critical frequency ν_c.

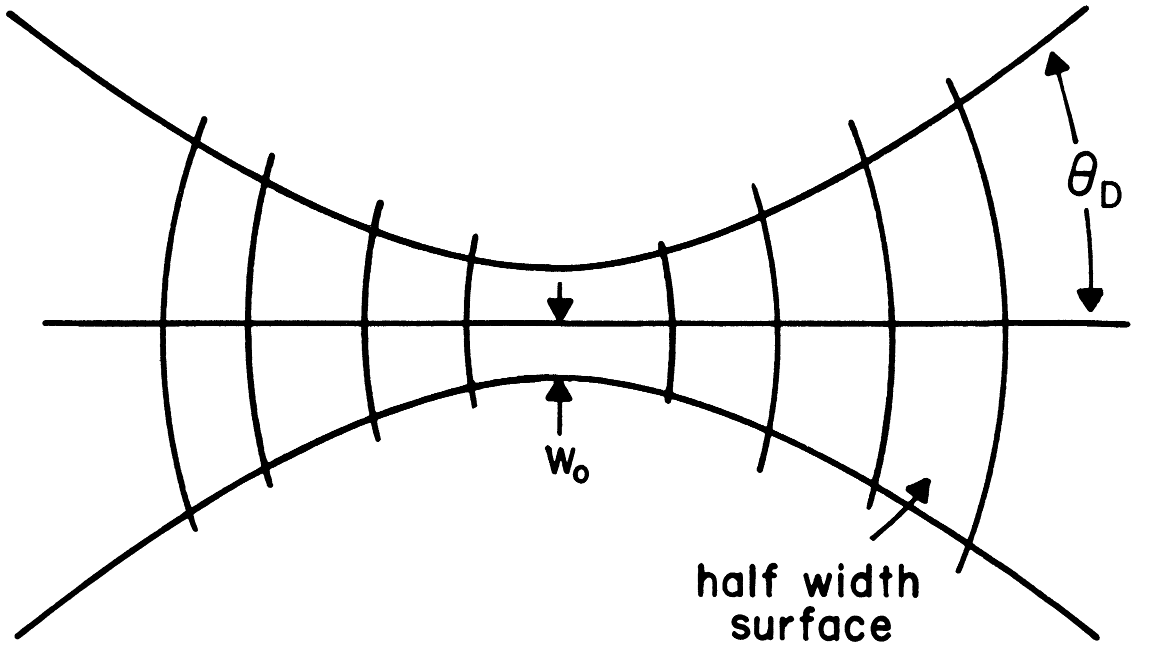

θD
Wo
half width surface

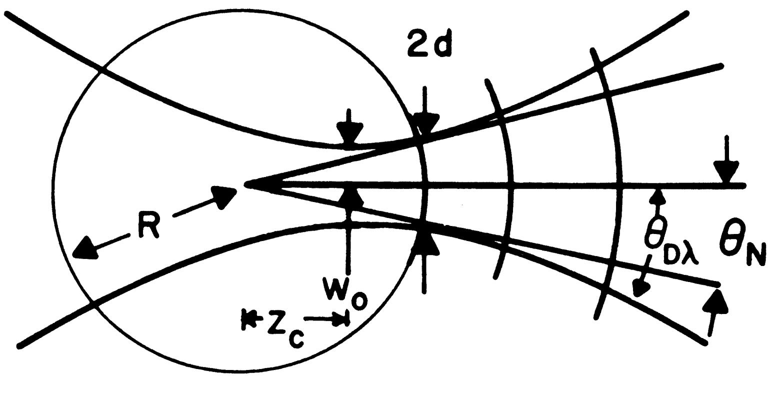

2d
R
Wo
Zc
θDλ
θN

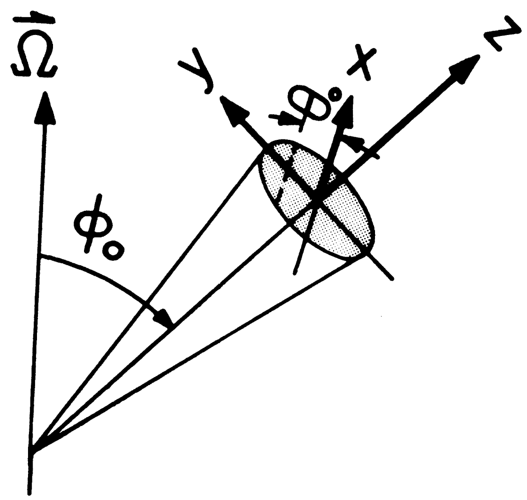

Fig. 3

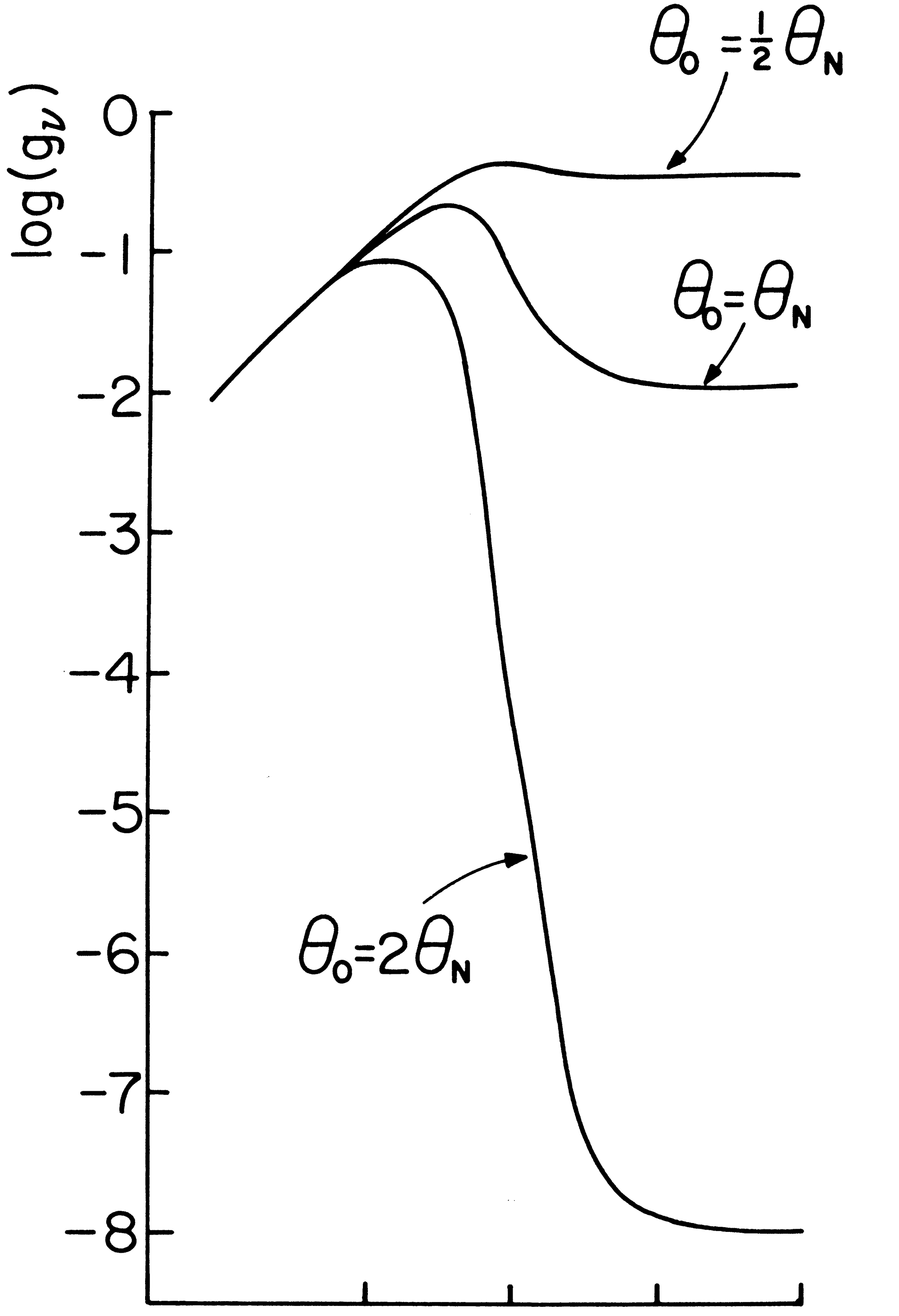

$\theta_0 = \frac{1}{2}\theta_N$
$\theta_0 = \theta_N$
$\theta_0 = 2\theta_N$
$\log(g_\nu)$
0
-1
-2
-3
-4
-5
-6
-7
-8
-1
0
1
2
$\log(\nu/\nu_c)$

Fig. 4